Chapter 7

Dynamics-Based Vibration Signal Modeling for Tooth Fault Diagnosis of Planetary Gearboxes

Xihui Liang, Ming J. Zuo and Wenhua Chen

Additional information is available at the end of the chapter

http://dx.doi.org/10.5772/67529

Abstract

Vibration analysis has been widely used to diagnose gear tooth fault inside a planetary gearbox. However, the vibration characteristics of a planetary gearbox are very complicated. Inside a planetary gearbox, there are multiple vibration sources as several sun-planet gear pairs, and several ring-planet gear pairs are meshing simultaneously. In addition, due to the rotation of the carrier, distance varies between vibration sources and a transducer installed on the planetary gearbox housing. Dynamics-based vibration signal modeling techniques can simulate the vibration signals of a planetary gearbox and reveal the signal generation mechanism and fault features effectively. However, these techniques are basically in the theoretical development stage. Comprehensive experimental validations are required for their future applications in real systems. This chapter describes the methodologies related to vibration signal modeling of a planetary gear set for gear tooth damage diagnosis. The main contents include gear mesh stiffness evaluation, gear tooth crack modeling, dynamic modeling of a planetary gear set, vibration source modeling, modeling of transmission path effect due to the rotation of the carrier, sensor perceived vibration signal modeling, and vibration signal decomposition techniques. The methods presented in this chapter can help understand the vibration properties of planetary gearboxes and give insights into developing new signal processing methods for gear tooth damage diagnosis.

Keywords: dynamic simulation, effect of transmission path, gear mesh stiffness, signal decomposition, fault diagnosis

1. Introduction

Planetary gearboxes are widely used in military and industrial applications. For example, they are main transmission components in military helicopters, wind turbines, and mining

trucks as shown in **Figure 1**. Comparing with fixed-shaft gearboxes, planetary gearboxes can afford higher torque load due to the load sharing among multiple gear pairs and generate larger transmission ratio with equal or smaller volume.

Figure 2 illustrates the structure of a one-stage planetary gear set that is composed of a sun gear, a ring gear, a carrier, and several planet gears. This planetary gear set can achieve multiple transmission scenarios as illustrated in **Table 1**. One transmission scenario can be selected in real applications based on individual application requirements. A planetary gear set is much more versatile in transmission scenarios comparing with a fixed-shaft gear set.

However, the versatility of planetary gearbox transmissions comes at a price: planetary gear sets are much more complicated to design and analyze. In the afternoon of April 1, 2009, a helicopter crashed into the North Sea and all 16 crew members died [1]. Later analysis concluded that this accident was caused by gear fatigue crack. Therefore, it is crucial to be able to detect early fault of planetary gearboxes; otherwise, large economic losses or catastrophes may occur. Vibration analysis, acoustic analysis, oil debris analysis, temperature analysis, and strain analysis are common techniques in the condition monitoring of gearbox systems. In this chapter, we only focus on the study of vibration analysis. Vibration analysis relies on the analysis of vibration signals to detect faults in a planetary gearbox.

There are mainly two ways to detect planetary gearbox damages based on vibration analysis. One way is to physically measure vibration responses of planetary gearboxes using vibration sensors and then analyze these vibration signals using advanced signal processing techniques to determine the health condition of planetary gearboxes [2–6]. **Figure 3** gives an example which is a planetary gearbox test rig located in the Department of Mechanical Engineering of the University of Alberta. Four types of experiments were performed in this test rig: gear tooth crack experiments, tooth pitting experiments, run-to-failure experiments, and various load and speed experiments [2]. Planetary gear fault detection/classification techniques were developed [3–6] by analyzing vibration signals collected from this experimental test rig. The second way is to model system responses (vibration signals) of planetary gearboxes using physical laws, like the Newton's laws of motion and then analyze simulated vibration signals aiming to reveal the nature of fault symptoms. The simulated vibration signals do not have the environmental noise interference. They can reveal fault features more easily than the physically measured signals. However, environmental noise did exist in real applications. The fault features revealed by the simulated signals may be submerged by the noise and

Figure 1. Applications of planetary gearboxes: (a) helicopter, (b) wind turbine, and (c) mining truck.

http://dx.doi.org/10.5772/67529

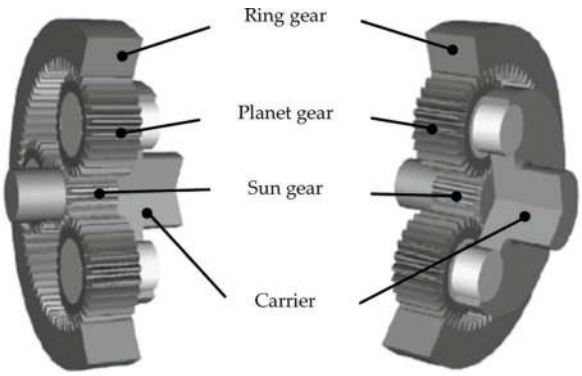

Figure 2. Structure of a planetary gear set.

Option	Inputs	Output
1	Sun (carrier fixed)	Ring
2	Ring (carrier fixed)	Sun
3	Carrier (sun fixed)	Ring
4	Ring (sun fixed)	Carrier
5	Sun (ring fixed)	Carrier
6	Carrier (ring fixed)	Sun
7	Sun and carrier	Ring
8	Ring and sun	Carrier
9	Ring and carrier	Sun

Table 1 Transmission scenarios of a planetary gear set as given in **Figure 2**.

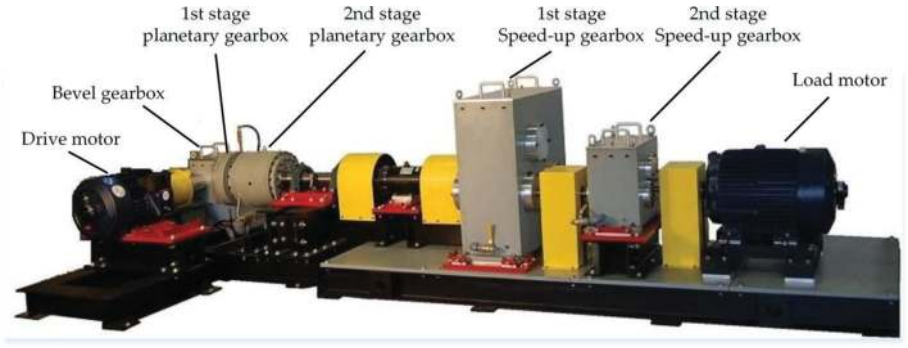

Figure 3. A planetary gearbox test rig located in the University of Alberta.

become ineffective. Therefore, environmental noise effect should be considered before applying the fault detection techniques developed using the simulated signals. In this chapter, we limit our focus on the second way of planetary gearbox modeling and fault diagnosis.

Three types of system responses can be obtained from analytical or numerical modeling of planetary gearboxes. The first type analysis mainly focuses on gear nature frequency and mode analysis [7–12]. The second type analysis is to analyze vibration properties of individual gears or dynamic forces of a gear pair among a planetary gear set [13–27]. In the first two types of analysis, the effect of gear transmission path is not considered. **Figure 4** illustrates three possible transmission paths for a vibration induced by a sun-planet meshing. Due to the effect of transmission path, some vibrations may be attenuated or submerged in the process of reaching a transducer located on the gearbox housing. Some researchers modeled the resultant vibration signals sensed by a transducer by considering multiple vibration sources inside a planetary gearbox and the effect of transmission path [5, 28–33]. A planetary gearbox has multiple vibration sources due to several sun-planet gear pairs and ring-planet gear pairs are meshing simultaneously. The effect of transmission path is mainly induced by the rotation of the carrier that causes the varying distance between a planet gear and a transducer mounted on the gearbox housing. The resultant vibration signals are the third type of system response. In the real applications, we generally install transducers on gearbox housing or bearing housing to collect vibration signals. Multiple vibration sources go through different transmission paths and reach the transducer. Therefore, it is important to consider both multiple vibration sources and the transmission path effect in vibration signal modeling. In this chapter, we focus on the modeling of resultant vibration signals of a planetary gearbox. An improved lumped parameter model [31] is used to simulate gearbox vibration source signals. This model is similar to the one reported in Ref. [7] with three distinctions: (1) the planet deflections are described in the horizontal and vertical coordinates, (2) both the gyroscopic force and the centrifugal force are incorporated, and (3) more accurate physical parameters are adopted. In addition, a modified Hamming function is used to model the effect of transmission path. This model is an improvement of widely used Hamming model [5, 28, 29]. The procedures to obtain resultant vibration signals are summarized in **Figure 5**. In the end, a new signal decomposition technique is used to enlarge gearbox fault signatures based on analysis of simulated vibration signals.

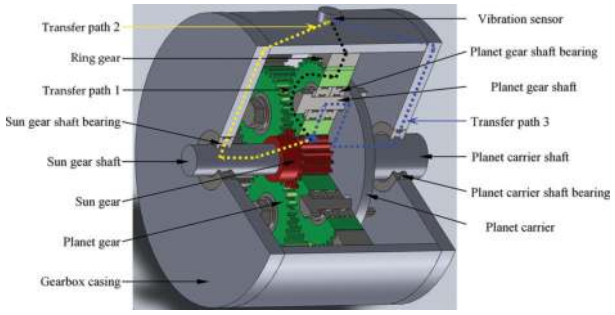

Figure 4. Transmission paths [5].

http://dx.doi.org/10.5772/67529

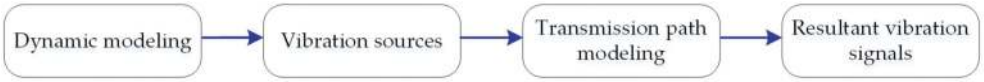

Figure 5. Procedures to obtain resultant vibration signals.

In this chapter, we present detailed procedures of modeling resultant vibration signals of a planetary gearbox with tooth damages and vibration signal decomposition techniques for fault diagnosis. Some challenges are described and analyzed. The remaining part of this chapter is organized as follows. In Section 2, a dynamic model is illustrated to simulate vibration source signals of a planetary gearbox. In Section 3, the methods to evaluate model parameters are described. In Section 4, the modeling of transmission path effect is given. Section 5 presents simulated vibration signals and fault symptoms. Section 6 describes vibration signal decomposition techniques for gear tooth damage diagnosis. Section 7 draws a summary and points out future research topics in dynamics-based vibration signal modeling and fault diagnosis of planetary gearboxes.

2. Dynamic modeling for simulation of vibration source signals

Planetary gearbox transmission systems are complex, and it is hard to consider all details of the transmission. As a result, people simplify the problem as much as possible while retaining all of the important and relevant features. A gearbox transmission can be modeled as a lumped system or a distributed system. A lumped system is simpler than a distributed system. A distributed system may be able to cover more details of a gearbox transmission, but its governing equations are hard to solve. The dependent variables of a lumped system are functions of time alone, and in general, the equation of motions is represented by ordinary differential equations. By contrast, the dependent variables of a distributed system are functions of time and one or more spatial variables, and the equation of motions can only be expressed by partial differential equations. Generally, the more details covered for a gearbox transmission system, the more complicated the equation of motions. Analytical solutions to complicated differential equations are hard to obtain. Numerical methods are mostly applied to solve them. However, four types of errors may be induced using numerical methods: round-off error, truncation error, accumulated error, and relative error [34]. It is time-consuming to solve complicated differential equations and sometimes it is even impossible to get a proper solution. Therefore, it is a trade-off between details to be covered and computation difficulties.

Figure 6 gives a typical modeling of a planetary gear set [30]. It is a 2D lumped parameter model. Each gear has three degrees of freedoms: angular rotation and transverse motions in the x- and y-directions. The gear mesh interface is modeled as a spring-damper system. Each bearing is also modeled as a spring-damper system. Other practical phenomena such as gear transmission error, backlash, tooth friction, gear shaft effect, gearbox housing effect, and gear misalignments are not considered in that model, but these can be selectively supplemented

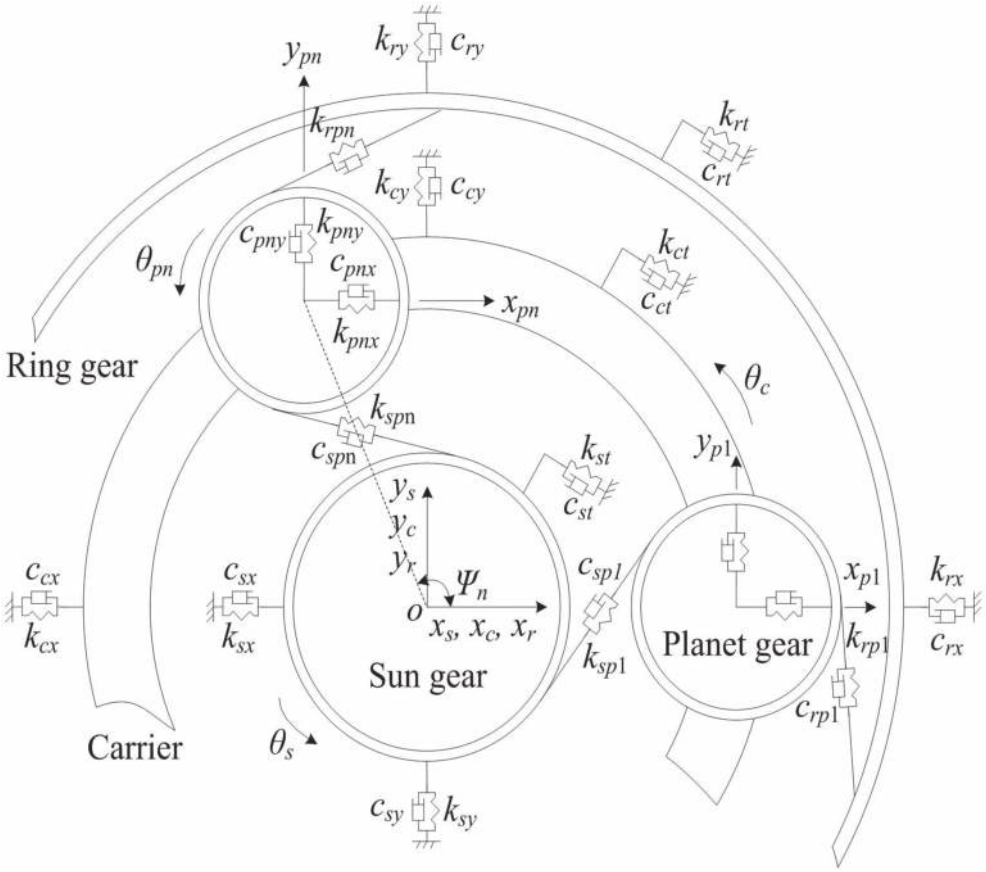

Figure 6. Modeling of a planetary gear set [30].

according to individual future research of interest. The model reported in Ref. [30] is used directly in this chapter to simulate vibration source signals of a planetary gearbox. The governing equations for this model are available in Ref. [30]. The vibration source signals will be illustrated later in Section 5.

3. Evaluation of physical parameters

For the dynamic model given in **Figure 6**, governing equations are available in Ref. [30]. But, several physical parameters in this model need to be evaluated before solving these equations, for example, gear mesh stiffness and damping, bearing stiffness and damping, and gear moment of inertia.

http://dx.doi.org/10.5772/67529

The most important one physical parameter is gear mesh stiffness. There are basically two ways to evaluate gear mesh stiffness: finite element method (FEM) and analytical method (AM). FEM is flexible to model any shaped gear and gear fault, but it is sensitive to contact tolerances, mesh density, and the type of finite elements selected. As the increase of mesh density, the numerical accuracy is improved, but the computation cost goes up. To reduce computation cost of FEM, Parker et al. [35] and Ambarisha and Parker [8] developed a combined element/contact mechanics model in gear mesh stiffness evaluation. Liang et al. [36] used linear finite element analysis to save computation cost in gear mesh stiffness evaluation. AM assumes a gear tooth as a nonuniform cantilever beam and beam theories are applied to evaluate gear mesh stiffness. AM has higher computational efficiency than FEM. But, AM is hard to model shape-complicated gear teeth and some gear faults. Potential energy method is one popular AM. This method has been used to evaluate mesh stiffness of perfect gears [37, 38], gears with crack [39–45], gears with a single tooth pit/spalling [46, 47], gears with multiple tooth pits [36], gears with a chipped tooth [39], gears with tooth plastic inclination deformation [19], gears with tooth profile modification [48], and gears with carrier misalignment errors [22].

In this section, the potential energy method used in Ref. [43] is illustrated to evaluate the mesh stiffness of a planetary gear set in healthy and cracked tooth conditions. The gear tooth is modeled as a nonuniform cantilever beam starting from gear base circle. The total energy stored in a pair of meshing gears is considered to be the summation of Hertzian contact energy, bending energy, shear energy, and axial compressive energy that corresponds to Hertzian contact stiffness, bending stiffness, shear stiffness, and axial compressive stiffness, respectively. When a gear tooth crack occurs, the effective tooth length, the area, and area moment of tooth sections of a cracked tooth are different from that of a perfect tooth, which leads to the gear mesh stiffness reduction. In Ref. [43], the gear tooth crack path is modeled in a straight line shape starting from the critical area of tooth root as shown in **Figure 7**. The critical area is around the maximum principle stress point at the tooth root. The equations for Hertzian contact stiffness (k_h), bending stiffness (k_b), shear stiffness (k_s), and axial compressive stiffness (k_a) are derived and available in Ref. [43]. These equations are expressed as a function of gear rotation angle (given gear geometry, material information, and crack information). Users can use these equations directly to evaluate gear mesh stiffness even though they are not familiar with beam and/or gear meshing theories. The total effective mesh stiffness k_t can be obtained as follows:

$$k_t = \sum_{i=1}^{m} \frac{1}{\frac{1}{k_{h,i}} + \frac{1}{k_{b1,i}} + \frac{1}{k_{s1,i}} + \frac{1}{k_{a1,i}} + \frac{1}{k_{b2,i}} + \frac{1}{k_{s2,i}} + \frac{1}{k_{a2,i}}} \tag{1}$$

where i represents the ith pair of meshing teeth and the subscripts 1 and 2 denote the driving gear and the driven gear, respectively.

Figure 8 summarizes the steps to obtain mesh stiffness of a planetary gear set. First, the mesh stiffness of a pair of sun-planet gears (a pair of external gears) and a pair of ring-planet gears (a pair of internal gears) should be evaluated using the potential energy method, respectively. Then, by incorporating gear mesh phase relationships [49], the mesh stiffness of other sun-planet gear pairs and ring-planet gear pairs can be obtained.

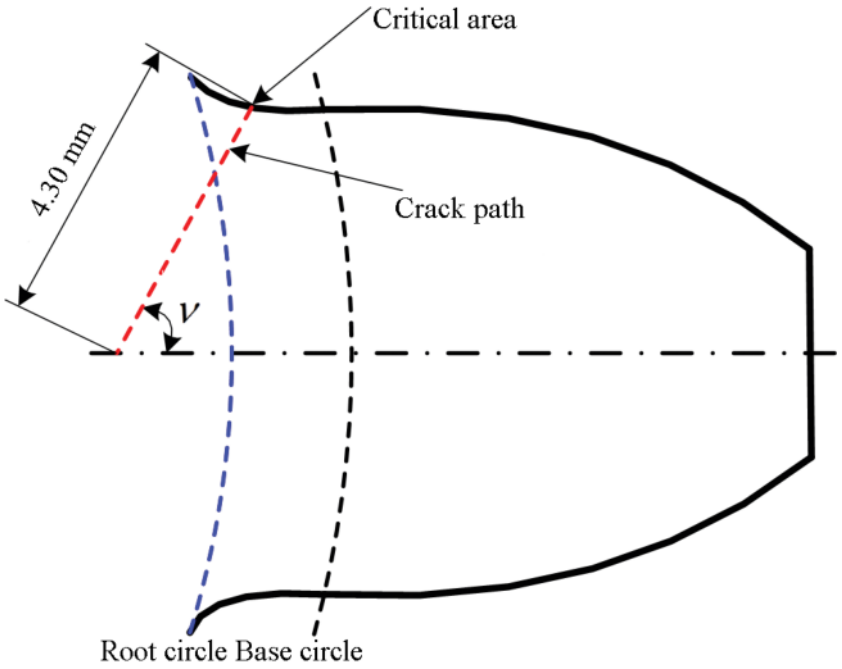

Figure 7. Tooth crack modeling.

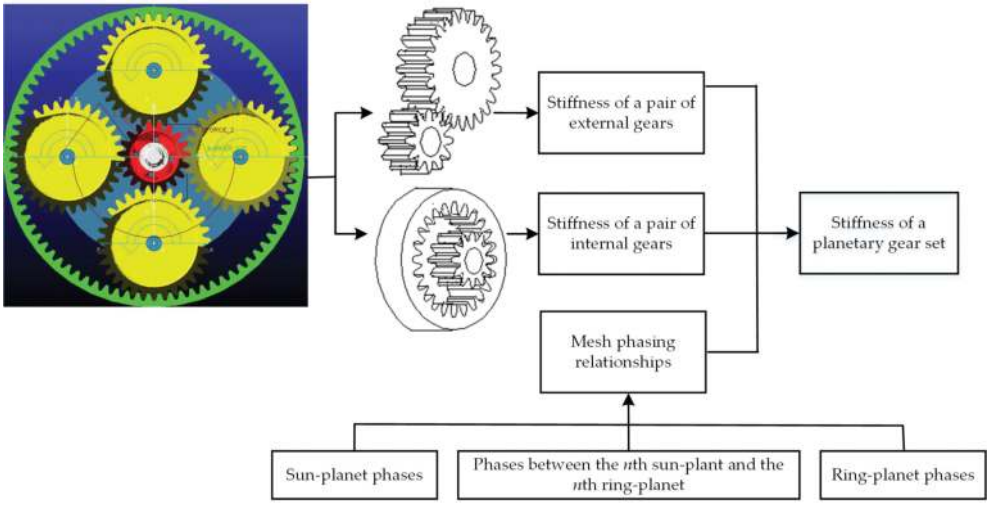

Figure 8. Steps to obtain mesh stiffness of a planetary gear set [31].

http://dx.doi.org/10.5772/67529

Table 2 gives the physical parameters of a planetary gear set. **Figure 9** illustrates the mesh stiffness of one sun-planet gear pair and one ring-planet gear pair of this planetary gear set using the method given in Ref. [43]. Two health conditions are given: perfect condition and 4.3 mm tooth crack condition. This crack length is illustrated in **Figure 7**. The tooth crack is in the planet gear (ring side). Under this scenario, the mesh stiffness of the sun-planet gear pair is assumed not to be affected by this planet gear tooth crack [43], while the mesh stiffness of the ring-planet gear pair reduces.

Parameters	Sun	Planets (4, equally spaced)	Ring
Number of teeth	19	31	81
Module (mm)	3.2	3.2	3.2
Pressure angle	20^o	20^o	20^o
Mass (kg)	0.700	1.822	5.982
Face width (m)	0.0381	0.0381	0.0381
Young's modulus (Pa)	2.068×10^{11}	2.068×10^{11}	2.068×10^{11}
Poisson's ratio	0.3	0.3	0.3
Base circle radius (mm)	28.3	46.2	120.8
Root circle radius (mm)	26.2	45.2	132.6
Reduction ratio	5.263		
Bearing stiffness	$k_{sx} = k_{sy} = k_{rx} = k_{ry} = k_{cx} = k_{cy} = k_{pmx} = k_{pmy} = 1.0 \times 10^8$ N/m		
Bearing damping	$c_{sx} = c_{sy} = c_{rx} = c_{ry} = c_{cx} = c_{cy} = c_{pmx} = c_{pmy} = 1.5 \times 10^3$ kg/s		

Table 2. Physical parameters of a planetary gear set [30].

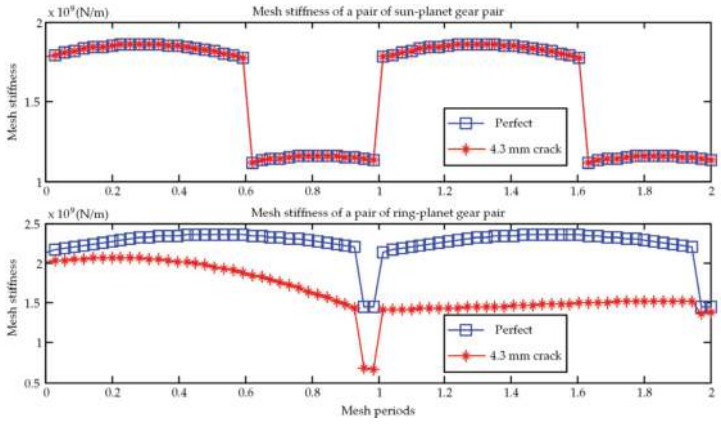

Figure 9. Mesh stiffness in perfect and cracked tooth conditions.

Similar methodology can be used to evaluate the effect of other gear faults like tooth pitting [36] on the mesh stiffness of a pair or gears. While many studies have been performed to evaluate gear mesh stiffness, the studies on the evaluation of gear mesh damping, bearing stiffness, and damping are rare. Gear mesh stiffness is assumed to be constant or proportional to gear mesh stiffness [40]. Bearing stiffness and damping are mostly assumed to be constant [30].

4. Modeling of transmission path effect

In **Figure 4**, three transmission paths are illustrated. However, most researchers only considered and modeled the effect of transmission path 1 since it has a shortest distance between vibration sources and the transducer. All researchers assumed that with the rotation of the carrier, the influence of a planet on vibration signals perceived by a transducer mounted on the gearbox housing reached its maximum when this planet was closest to the transducer; then this planet's influence decreased as the planet went away from the transducer. The transmission path effect model is assumed to be independent of gear fault modes. It can be used for gear tooth crack, pitting, spalling, wear, and so on. A Hanning function was used in Refs. [28, 29], and a Hamming function was used in Refs. [32, 50] to represent the effect of transmission path. A modified Hamming function with adjustable window bandwidth was proposed in Ref. [30]. Liu et al. [33] used the modified Hamming function to model the transmission path along the casing and also proposed two constants to represent the transmission path inside the casing. In this study, the modified Hamming function reported in Ref. [30] is used to represent the effect of transmission path. The resultant vibration $a(t)$ is modeled as the summation of weighted vibration of each planet gear as follows:

$$a(t) = \sum_{n=1}^{N} e^{a\left(\mathrm{mod}\left(w_c t+\phi,2\pi\right)-\pi\right)^2} H_m(t)\, a_n(t) \tag{2}$$

where N represents the number of planet gears, w_c denotes carrier rotation speed, ϕ represents circumferential angle of the nth planet gear, $H_m(t)$ is the Hamming function, $a_n(t)$ represents the acceleration signal of the nth planet gear, and the parameter a is used to control bandwidth of a Hamming function.

5. Vibration signal analysis and fault symptoms

Figure 10 gives the vertical acceleration signals of a single planet gear under healthy and cracked tooth conditions. The large spikes on this figure are generated by the meshing of the cracked tooth. The angular interval of these large spikes is 31 θ_m where θ_m represents the rotation angle of a planet gear in one tooth mesh period. The ring gear has 81 teeth, and therefore, in one revolution of the carrier, a planet gear's angular displacement is 81 θ_m.

Figure 11 shows the resultant vibration signals of a planet gearbox obtained using Eq. (2). Amplitude modulation can be observed from resultant vibration signals because four planet

http://dx.doi.org/10.5772/67529

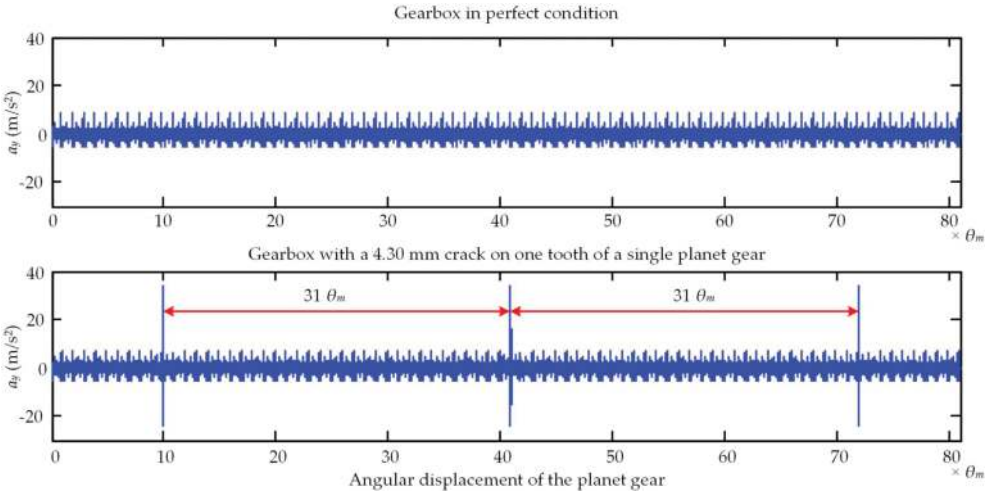

Figure 10. Vibration of a single planet gear.

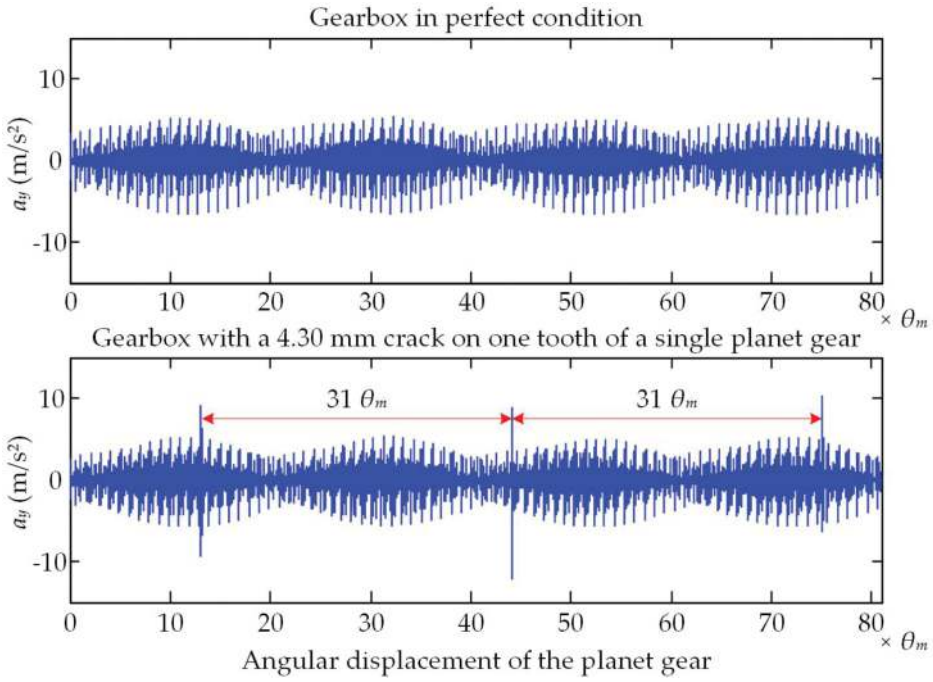

Figure 11. Resultant vibration of a planetary gearbox [31].

gears pass through the transducer sequentially in one revolution of the carrier and their effects on resultant vibration signals vary according to their locations. The amplitude of resultant vibration signals is smaller than that of a single planet gear because some vibration signals are attenuated during transmission. The amplitude of large spikes generated by the cracked tooth varies largely because the signal attenuation is not uniform. The farther between a planet gear and a transducer, the larger signal attenuation for this planet gear.

Similarly, for other types of planetary gear faults, the resultant vibration signals can be simulated by considering both vibration source signals and the effect of transmission path. The vibration source signals are related to gear faults by a dynamic model. The transmission path effect model is irrelevant with gear faults.

6. Vibration signal decomposition for fault diagnosis

From **Figure 11**, we can see that the time duration of large spikes generated by the cracked tooth is very short. These large spikes are not such obvious in experimental signals because of noise pollution [31]. Actually, they are very weak according to the experimental findings in Ref. [30, 31]. Therefore, people proposed signal decomposition techniques to enlarge the fault symptoms generated by a damaged gear tooth. In Ref. [51], McFadden used a window function to sample the vibration signals of a planetary gearbox when the planet gear of interest was passing the transducer and then the signal samples were mapped to the corresponding teeth of the sun gear or a planet gear to construct the vibration signals of the sun gear or a planet gear. The decomposed signal reduces the interference from other gear vibrations and emphasizes the fault symptoms of the gear of interest. Liang et al. [31] proposed another windowing and mapping strategy to generate the vibration signal of each tooth of the planet gear of interest. If a planet gear has N teeth, the resultant vibration signal can be decomposed into N subsignals. Each subsignal corresponds to one tooth. Examining the differences of these N subsignals, the health differences of these N teeth can be measured. The detailed signal decomposition techniques will not be described in detail in this chapter as they are available in the published papers [31, 51]. **Figure 12** illustrates the effectiveness of the windowing and mapping strategy proposed in Ref. [31]. **Figure 12(a)** gives the resultant vibration signal of a planetary gearbox with a single tooth crack on a planet gear. **Figure 12(b)** and **(c)** illustrate the decomposed vibration signals according to a perfect tooth and the cracked tooth, respectively. More obvious fault symptoms can be observed from **Figure 12(c)** than the original resultant vibration signal as shown in **Figure 12(a)**. Examining the differences between **Figure 12(b)** and **(c)**, it is easy to tell that **Figure 12(c)** is generated by a cracked tooth.

This vibration signal decomposition technique [31] is able to identify the tooth health condition differences. If some teeth are in healthy condition while others are in damaged condition, this method will be effective for fault diagnosis. In an extreme case, if all gear teeth have the same damage severity, like evenly distributed pitting, this method will be ineffective as there is no difference between the health conditions of teeth.

http://dx.doi.org/10.5772/67529

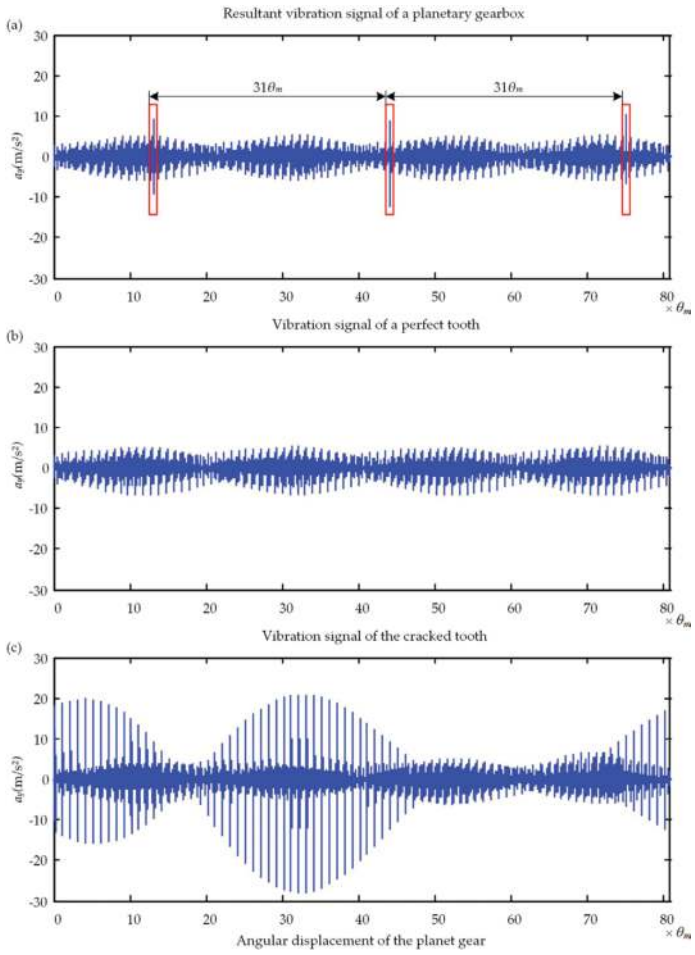

Figure 12. Vibration signal decomposition of a planetary gearbox [31]: (a) resultant vibration signal, (b) decomposed signal for a perfect tooth, and (c) decomposed signal for a cracked tooth.

7. Summary and future work

This chapter describes techniques for dynamics-based vibration signal modeling and fault diagnosis of planetary gearboxes. The planetary gearbox vibration signal modeling contains two parts: the simulation of vibration source signals and the modeling of transmission path effect. The current research status and challenges of dynamic modeling-based fault diagnosis are introduced. In the example given in this chapter, vibration source signals are obtained by a lumped parameter dynamic model, the gear fault is reflected by the time-varying mesh stiffness which is evaluated using the potential energy method, and the effect of transmission path is modeled using a modified Hamming function. Other window functions are also

described to model the effect of transmission path. However, further researches to test and validate these window functions are required. In the end, vibration decomposition techniques are briefly described for gear tooth damage diagnosis. Comparing between the raw signal and the decomposed signal, we can find that the signal decomposition technique can enlarge gearbox fault symptoms and facilitate fault diagnosis.

Based on the research scope of this chapter, the following perspectives are suggested for future consideration:

(1) Mesh stiffness evaluation with crack/pitting in multiple teeth.

(2) Mesh stiffness evaluation with multiple fault modes.

(3) Experimental validation of methods in evaluating gear mesh stiffness.

(4) Gear mesh damping evaluation.

(5) Bearing stiffness and damping evaluation.

(6) Time-varying load or random load effect on the vibration signals.

(7) Experimental validation of models for transmission path effects.

(8) Effects of noises from internal and/or external sources.

(9) Dynamic and vibration properties of gearboxes with multiple faults (multiple fault locations and/or multiple fault modes).

(10) Development of fault diagnosis techniques based on the understanding of vibration properties.

Acknowledgements

This research is supported by the Natural Science and Engineering Research Council of Canada, Canada (Grant No. RGPIN-2015-04897); the International S&T Cooperation Program of China, China (Grant No. 2015DFA71400); the National Natural Science Foundation of China, China (Grant No. 51375078 and No. 51505066); the ConocoPhillips Canada Limited Graduate Scholarship, Canada; and the American Gear Manufacturers Association Foundation Scholarship, USA.

Author details

Xihui Liang[1], Ming J. Zuo[1]* and Wenhua Chen[2]

*Address all correspondence to: ming.zuo@ualberta.ca

1 Department of Mechanical Engineering, University of Alberta, Edmonton, Alberta, Canada

2 Key Laboratory of Reliability Technology for Mechanical and Electrical Product of Zhejiang Province, Zhejiang Sci-Tech University, Hangzhou, China

References

[1] The Guardian. North Sea helicopter crash report says gearbox failed after maintenance error [Internet]. 2011. Available from: https://www.theguardian.com/uk/2011/nov/24/north-sea-helicopter-crash-report [Accessed: 2017-02-14]

[2] Hoseini MR, Lei Y, Tuan DV, Patel T, Zuo MJ. *Experiment design of four types of experiments: pitting experiments, run-to-failure experiments, various load and speed experiments, and crack experiments*. Technical Report, Reliability Research Lab, Mechanical Department, University of Alberta, Edmonton, Alberta, Canada, January 2011.

[3] Zhao X, Zuo MJ, Liu Z, Hoseini MR. Diagnosis of artificially created surface damage levels of planet gear teeth using ordinal ranking. *Measurement* 2013; 46: 132–144.

[4] Liu Z, Qu J, Zuo MJ, Xu H. Fault level diagnosis for planetary gearboxes using hybrid kernel feature selection and kernel fisher discriminant analysis. *Int J Adv Manuf Technol* 2012; 67: 1217–1230.

[5] Feng Z, Zuo MJ. Vibration signal models for fault diagnosis of planetary gearboxes. *J Sound Vib* 2012; 331: 4919–4939.

[6] Feng Z, Zuo MJ. Fault diagnosis of planetary gearboxes via torsional vibration signal analysis. *Mech Syst Signal Process* 2013; 36: 401–421.

[7] Lin J, Parker RG. Analytical characterization of the unique properties of planetary gear free vibration. *J Vib Acoust* 1999; 121: 316–321.

[8] Ambarisha VK, Parker RG. Nonlinear dynamics of planetary gears using analytical and finite element models. *J Sound Vib* 2007; 302: 577–595.

[9] Bahk C-J, Parker RG. Analytical solution for the nonlinear dynamics of planetary gears. *J Comput Nonlinear Dyn* 2011; 6: 21007.

[10] Parker RG. A physical explanation for the effectiveness of planet phasing to suppress planetary gear vibration. *J Sound Vib* 2000; 236: 561–573.

[11] Ericson T, Parker RG. Planetary gear modal properties and dynamic response: experiments and analytical simulation. In: *ASME 2011 International Design Engineering Technical Conferences and Computers and Information in Engineering Conference*. American Society of Mechanical Engineers, Columbus, Ohio, USA, 2011. p. 331–343.

[12] Ericson TM, Parker RG. Planetary gear modal vibration experiments and correlation against lumped-parameter and finite element models. *J Sound Vib* 2013; 332: 2350–2375.

[13] Al-shyyab A, Kahraman A. A non-linear dynamic model for planetary gear sets. *Proc Inst Mech Eng Part K J Multi-Body Dyn* 2007; 221: 567–576.

[14] Inalpolat M, Kahraman A. Dynamic modelling of planetary gears of automatic transmissions. *Proc Inst Mech Eng Part K J Multi-Body Dyn* 2008; 222: 229–242.

[15] Yuksel C, Kahraman A. Dynamic tooth loads of planetary gear sets having tooth profile wear. *Mech Mach Theory* 2004; 39: 695–715.

[16] Kahraman A. Load sharing characteristics of planetary transmissions. *Mech Mach Theory* 1994; 29: 1151–1165.

[17] Kahraman A Planetary gear train dynamics. *J Mech Des* 1994; 116: 713–720.

[18] Chen Z, Shao Y. Dynamic features of a planetary gear system with tooth crack under different sizes and inclination angles. *J Vib Acoust* 2013; 135: 1–12.

[19] Shao Y, Chen Z. Dynamic features of planetary gear set with tooth plastic inclination deformation due to tooth root crack. *Nonlinear Dyn* 2013; 74: 1253–1266.

[20] Chen Z, Shao Y. Dynamic simulation of planetary gear with tooth root crack in ring gear. *Eng Fail Anal* 2013; 31: 8–18.

[21] Cheng Z, Hu N, Zhang X. Crack level estimation approach for planetary gearbox based on simulation signal and GRA. *J Sound Vib* 2012; 331: 5853–5863.

[22] Cao Z, Shao Y, Zuo MJ, Liang X. Dynamic and quasi-static modeling of planetary gear set considering carrier misalignment error and varying line of action along tooth width. *Proc Inst Mech Eng Part C J Mech Eng Sci* 2015; 229: 1348–1360.

[23] Cheng Z, Hu N, Gu F, Qin G. Pitting damage levels estimation for planetary gear sets based on model simulation and grey relational analysis. *Trans Can Soc Mech Eng* 2011; 35: 403–417.

[24] Li G, Li F, Wang Y, Dong D. Fault diagnosis for a multistage planetary gear set using model-based simulation and experimental investigation. *Shock Vib* 2016; 2016: 1–19.

[25] Chaari F, Fakhfakh T, Haddar M. Dynamic analysis of a planetary gear failure caused by tooth pitting and cracking. *J Fail Anal Prev* 2006; 6: 73–78.

[26] Chaari F, Hbaieb R, Fakhfakh T, Haddar M. Dynamic response simulation of planetary gears by the iterative spectral method. *Int J Simul Model* 2005; 4: 35–45.

[27] Chaari F, Fakhfakh T, Hbaieb R, Louati J, Haddar M. Influence of manufacturing errors on the dynamic behavior of planetary gears. *Int J Adv Manuf Technol* 2006; 27: 738–746.

[28] Inalpolat M, Kahraman A. A theoretical and experimental investigation of modulation sidebands of planetary gear sets. *J Sound Vib* 2009; 323: 677–696.

[29] Inalpolat M, Kahraman A. A dynamic model to predict modulation sidebands of a planetary gear set having manufacturing errors. *J Sound Vib* 2010; 329: 371–393.

[30] Liang X, Zuo MJ, Hoseini MR. Vibration signal modeling of a planetary gear set for tooth crack detection. *Eng Fail Anal* 2015; 48: 185–200.

[31] Liang X, Zuo MJ, Liu L. A windowing and mapping strategy for gear tooth fault detection of a planetary gearbox. *Mech Syst Signal Process* 2016; 80: 445–459.

[32] Liang X, Zuo MJ. *Investigating Vibration Properties of a Planetary Gear Set with a Cracked Tooth in a Planet Gear*. Fort Worth, Texas, USA, 2014. p. 568–575.

[33] Liu L, Liang X, Zuo MJ. Vibration signal modeling of a planetary gear set with transmission path effect analysis. *Measurement* 2016; 85: 20–31.

[34] Ritger PD, Rose NJ. *Differential equations with applications*. Courier Corporation, USA 1968.

[35] Parker RG, Vijaykar SM, Imajo T. Non-linear dynamic response of a spur gear pair: modelling and experimental comparisons. *J Sound Vib* 2000; 237: 435–455.

[36] Liang X, Zhang H, Liu L, Zuo MJ. The influence of tooth pitting on the mesh stiffness of a pair of external spur gears. *Mech Mach Theory* 2016; 106: 1–15.

[37] Yang DCH, Lin JY. Hertzian damping, tooth friction and bending elasticity in gear impact dynamics. *J Mech Des* 1987; 109: 189–196.

[38] Liang X, Zuo MJ, Patel TH. Evaluating the time-varying mesh stiffness of a planetary gear set using the potential energy method. *Proc Inst Mech Eng Part C J Mech Eng Sci* 2014; 228: 535–547.

[39] Tian X, Zuo MJ, Fyfe KR. Analysis of the Vibration Response of a Gearbox with Gear Tooth Faults. Anaheim, California, USA, 2004. p. 785–793.

[40] Wu S, Zuo MJ, Parey A. Simulation of spur gear dynamics and estimation of fault growth. *J Sound Vib* 2008; 317: 608–624.

[41] Chen Z, Shao Y. Dynamic simulation of spur gear with tooth root crack propagating along tooth width and crack depth. *Eng Fail Anal* 2011; 18: 2149–2164.

[42] Pandya Y, Parey A. Failure path based modified gear mesh stiffness for spur gear pair with tooth root crack. *Eng Fail Anal* 2013; 27: 286–296.

[43] Liang X, Zuo MJ, Pandey M. Analytically evaluating the influence of crack on the mesh stiffness of a planetary gear set. *Mech Mach Theory* 2014; 76: 20–38.

[44] Ma H, Song R, Pang X, et al. Time-varying mesh stiffness calculation of cracked spur gears. *Eng Fail Anal* 2014; 44: 179–194.

[45] Ma H, Pang X, Zeng J, Wang Q, Wen B. Effects of gear crack propagation paths on vibration responses of the perforated gear system. *Mech Syst Signal Process* 2015; 62–63: 113–128.

[46] Abouel-seoud SA, Dyab ES, Elmorsy MS. Influence of tooth pitting and cracking on gear meshing stiffness and dynamic response of wind turbine gearbox. *Int J Sci Adv Technol* 2012; 2: 151–165.

[47] Ma H, Li Z, Feng M, Feng R, Wen B. Time-varying mesh stiffness calculation of spur gears with spalling defect. *Eng Fail Anal* 2016;66: 166–176.

[48] Chen Z, Shao Y. Mesh stiffness calculation of a spur gear pair with tooth profile modification and tooth root crack. *Mech Mach Theory* 2013;62: 63–74.

[49] Parker RG, Lin J. Mesh phasing relationships in planetary and epicyclic gears. *J Mech Des* 2004; 126: 365–370.

[50] Liang X, Zuo MJ, Hoseini MR. Understanding vibration properties of a planetary gear set for fault detection. In: *2014 IEEE Conference on Prognostics and Health Management (PHM)*. 2014, pp. 1–6.

[51] McFadden PD. A technique for calculating the time domain averages of the vibration of the individual planet gears and the sun gear in an epicyclic gearbox. *J Sound Vib* 1991; 144: 163–172.